DOI: 10.1111/eci.12667

ORIGINAL ARTICLE

Dying blood mononuclear cell secretome exerts antimicrobial activity

Mohammad Mahdi Kasiri[*], Lucian Beer[*,†], Lucas Nemec[‡], Florian Gruber[§,¶], Sabine Pietkiewicz[**], Thomas Haider[*], Elisabeth Maria Simader[*], Denise Traxler[*], Thomas Schweiger[‡], Stefan Janik[*], Shahrokh Taghavi[‡], Christian Gabriel[††], Michael Mildner[§] and Hendrik Jan Ankersmit[*,‡,‡‡]

[*]Christian Doppler Laboratory for Cardiac and Thoracic Diagnosis and Regeneration, Vienna, Austria, [†]Department of Biomedical Imaging and Image-guided Therapy, [‡]Division of Thoracic Surgery, [§]Department of Dermatology, Medical University of Vienna, Vienna, Austria, [¶]Christian Doppler Laboratory for Biotechnology of Skin Aging, Vienna, Austria, [**]Translational Inflammation Research, Otto von Guericke University, Magdeburg, Germany, [††]Red Cross Blood Transfusion Service of Upper Austria, Linz, Austria, [‡‡]Head FFG Project 852748 'APOSEC', Medical University of Vienna, Vienna, Austria

ABSTRACT

Background Several activities are attributed to antimicrobial peptides (AMPs), including bacterial killing, leucocyte recruitment and angiogenesis. Despite promises of advanced cellular therapies for treatment of diabetic foot ulcer, it is currently accepted that paracrine factors rather than cellular components are causative for the observed effects. Whether AMPs are present in the mononuclear cell (MNC) secretome (MNC-sec) of white blood cells that are beneficial in experimental wound healing is not known.

Materials and methods Antimicrobial activity of the secretomes of nonirradiated (MNC-sec) and γ-irradiated MNCs (MNC-sec rad) was analysed by microdilution assay. AMPs were determined by quantitative real-time PCR (RT-PCR) and enzyme-linked immunosorbent assay (ELISA). Whether human MNC-sec rad causes AMP secretion *in vivo* was examined in an experimental rat model. Image flow cytometry was used to determine the type of cell death induced in MNCs after exposure to γ-radiation.

Results The antimicrobial activity assay revealed a bactericidal activity of MNC-sec rad and to a lesser degree also of MNC-sec. Image flow cytometry showed that γ-irradiation of MNCs induced early apoptosis followed mainly by necroptosis. RT-PCR and ELISA revealed a high abundance of different AMPs in the secretome of MNCs. In addition, human MNC-sec elicited an increase in *de novo* endogenous AMP production in rats *in vivo*.

Conclusion We provide evidence that the secretome of MNCs has direct and indirect positive effects on the immune defence system, including augmentation of antibacterial properties. Our data further suggest that necroptosis could play a key role for the release of paracrine factors and the therapeutic action of MNC-sec rad.

Keywords Antimicrobial peptides, diabetic foot ulcer, MNC secretome, mononuclear cell, peripheral blood mononuclear cells.

Eur J Clin Invest 2016; 46 (10): 853–863

Introduction

Antimicrobial peptides (AMPs) are part of the innate immunity with broad-spectrum activity against bacteria and fungi. Among several activities attributed to them, chemotactic properties such as recruitment of other leucocytes along with direct bacterial killing have been investigated [1,2]. Several groups have proposed them as offering a promising new approach to common antibiotic therapies in the case of bacterial resistance [3] or nonhealing wounds like diabetic foot ulcer (DFU) [4]. According to recent reports, DFUs are infected in the majority of cases [5,6], and one in six patients requires amputation; however, successful treatment of DFU highly depends on complex events, including adequate angiogenesis or antibacterial actions [7,8].

Advanced cellular therapies hold promise as therapeutic agents for their known antimicrobial activity [9], angiogenesis [10] and wound healing [11]. Several studies have shown that mesenchymal stem cells (MSCs) represent an effective therapeutic agent in a variety of experimental models. For instance, Maharlooei *et al.* [12] showed that adipose tissue-derived MSCs enhance diabetic wound healing in a diabetic rat model. Krasnodembskaya *et al.* studied the effect of human bone marrow-derived MSCs on the bacterial growth of

Gram-negative and Gram-positive bacteria. They showed that MSCs and their conditioned medium both have inhibitory effects on bacterial growth [9]. The idea of therapeutically using the secretome of MNCs originates from stem cell research results and suggests that the observed beneficial effects of stem cell therapy are due to paracrine factors rather than direct cellular components [13]. In this study, we focused on secretomes derived from living (MNC-sec) or dying (MNC-sec rad) peripheral blood MNCs which Korf-Klingebiel *et al.* [14] showed is only moderately different from the stem cell secretome.

Previously, our group identified the following effects of MNC-sec rad in preclinical investigations: (i) regeneration of infarcted myocardium in an acute myocardial infarction (AMI) model [15]; (ii) reduction in microvascular obstruction after AMI [16]; (iii) protection against autoimmune myocarditis [17]; (iv) reduction in infarction area in a preclinical stroke model [18]; and (v) enhancement of wound healing in a murine model of wound healing [19].

Agerberth *et al.* [20] showed that some AMPs are expressed by specific lymphocyte and monocyte populations from MNCs and can be enhanced by proinflammatory cytokines *in vitro*. Mildner *et al.* [19] reported that MNC-sec can improve wound healing in a murine model *in vitro*. Moreover, and more relevant to the human wound setting, we showed that the topical application of irradiated MNC-sec improves the quality of the regenerating skin and increases angiogenesis in the wound area in a porcine burn injury and skin grafting model [21].

In 2014, we began a first secretome-based regenerative Phase I study to investigate the safety and tolerability of topically administered autologous good manufacturing practice (GMP) protocol MNC secretome (ApoSec; Marsyas I clinical trial; EudraCT Nr.: 2013-000756-17; NCT02284360). This trial is intended as a first step towards a clinical proof-of-concept study of DFU patients (Phase II). Because treatment of DFUs is complicated by its poly-factorial pathogenesis, including polymicrobial infection in the wound area, we became interested in whether MNC-sec also comprises antimicrobial activities. To address this question, we produced MNC-sec rad under GMP conditions and investigated AMP content and functional activity *in vitro* and *in vivo*. Our preclinical data support the notion that MNC-sec rad is able to directly kill bacterial pathogens, a much desired effect in the treatment of DFU.

Material and methods

Internal review board and ethics

This study and all experimental procedures were approved by the ethics committee of the Medical University of Vienna (vote number: 1236; 2013) and conducted according to the principles of the Helsinki Declaration and Good Clinical Practice. Written informed consent was obtained from all participants aged 18–40 years. Exclusion criteria were any treatment with immunomodulatory medication during the past 4 weeks and any signs of acute infection. All animal procedures were approved by the Animal Research Committee of the Medical University of Vienna (Prot. Nr.: 66·009/0220WF/II/3b/2014).

MNC-sec preparation

Human MNC secretome were prepared as described previously by Beer *et al* [22.], Irradiated and nonirradiated MNCs and their supernatants were collected separately after 0, 4 and 24 h of incubation and served as experimental groups.

Production of MNC secretome from humans and control medium according to good manufacturing practice protocol for experimental setting

Human GMP MNC-sec samples were prepared as described previously by Altmann *et al.* [18].

Investigation of cell death by ImageStream analysis. We adapted the method described by Pietkiewicz *et al.* for the FlowSight(R) cytometer to the ImageStream (Amnis(R), part of EMD Millipore, MilliporeSigma, The life science business of Merck KGaA, Darmstadt, Germany) cytometer. In brief, cells were stained with AnnexinV FLUOS and propidium iodide (Annexin V –FLUOS staining kit; Roche Diagnostics, Basel, Switzerland) in incubation buffer according to the manufacturer's instructions and analysed immediately. In the flow cytometer, debris and doublets were gated out, and focused cells that were excited with the 488 nm laser were used for analysis. Per condition, at least 20 000 events (=pictures) were recorded in the bright field (430–480 nm), Annexin V- FLUOS (505–560 nm) and PI (430–480 nm) channels. Colour compensation from single-labelled samples was performed as described before [23]. For analysis, IDEAS 6.2 software (MilliporeSigma) was used, and focused, single cells were identified using the gradient root mean square (RMS) of the BF image, followed by bright field image area and aspect ratio intensity. The fluorescence intensity of Annexin V-FLUOS and PI allowed to distinguish between double negative (live and healthy) cells, Annexin V-positive (early apoptotic) cells and double-positive cells that can either be late apoptotic or necroptotic. By applying the image-based features 'intensity threshold [> 30%]' and 'contrast morphology' for the PI channel as described in Pietkiewicz *et al.* [23], we could distinguish between late apoptotic (small fragmented nuclei) and necroptotic cells (nonfragmented enlarged nuclei).

Total RNA isolation and quantitative real-time polymerase chain reaction

Total RNA isolation and quantitative real-time polymerase chain reaction (qPCR) were performed as described previously

by Beer *et al.* [22]. The following primer pairs were used: forward primer 5′-AGAAGCGGGTGAGAAACAAA-3′ and reverse primer 5′-TGTGGCTCGGTACTGGCATG-3′ for Angiogenin/RNase5; forward primer 5′-CAGCTGGAACGCA ACATAGA-3′ and reverse primer 5′-TCAGCTGCTTGTCTGCA TTT-3′ for S100A9; forward primer 5′-GCTAACCTCTAC CGCCTCCT-3′ and reverse primer 5′-GGTCACTGTCCCCATA CACC-3′ for cathelicidin; forward primer 5′- GAGTCACAGCA CGAAGACCA-3′ and reverse primer 5′- GGCTGCATGTGC TGAATTT-3′ for RNase7; and forward primer 5′-GATGAGT ATGCCTGCCGTGTG-3′ and reverse primer 5′-CAATCCA AATGCGGCATCT-3′ for B2M. The relative expression of target genes was compared to the housekeeping gene B2M using a formula described by Pfaff *et al* [24.]

AMP enzyme-linked immunosorbent assay analysis of human experimental/GMP MNC-sec and rat serum

AMP levels were measured using commercially available enzyme-linked immunosorbent assay (ELISA) kits, following the manufacturers' instructions (human beta-defensin 124: catalog# SEQ656Hu; human ribonuclease A3: catalog# SEB758Hu; all Uscn Life Science, Wuhan, China; human LL-37, cathelicidin: catalog# HK321; human calprotectin: catalog# HK325; all Hycult Biotech, Uden, the Netherlands; human angiogenin, RNase5: catalog# DY265 R&D Systems, Minneapolis, MN, USA; and rat calprotectin: catalog# HK321; Immundiagnostik AG, Bensheim, Germany). Optical density values were measured at 450 nm on an ELISA plate reader (Victor3 multilabel plate reader; PerkinElmer, Waltham, MA, USA).

Antimicrobial assay and MNC-sec

The antimicrobial potency of MNC-sec was determined by a microdilution assay [25] using the following pathogens: *Pseudomonas aeruginosa* (ATCC 27853), *Escherichia coli* (ATCC 11303), *Staphylococcus aureus* (ATCC 33592) and *Streptococcus pyogenes*. Pathogens were incubated for 3 h with the secretome of irradiated MNCs (250×10^6) at 37 °C. Thereafter, suspensions were diluted and applied to Columbia agar plates with 5% sheep blood. The antibiotic activity was analysed by determination of the number of colony-forming units the next day. The protocol of the bacterial assay is presented in detail in Appendix 1.

Furthermore, we investigated the antimicrobial activity of MNC-sec after blocking two of the major AMPs by neutralizing antibodies. The following antibodies were used for blocking experiments: Angiogenin/RNAse5 (LSBio, Seattle, WA, USA; clone 27E10, 25 μg/mL) and Calprotectin (Santa Cruz, Dallas, TX USA; clone D-5, 25 μg/mL).

Rat AMP secretion after exposure to the human GMP MNC secretome

Adult male Sprague–Dawley rats weighing between 300 and 350 g ($n = 21$, Department of Biomedical Research, Medical University of Vienna, Austria) were used for our experiments and housed under standard conditions. In the experiments, the animals were anesthetized with 1·5% isoflurane to assure proper intraperitoneal (i.p.) application of medium or GMP MNC-sec. Animals were divided into one Medium and one MNC-sec rad group and received 1 mL of Medium or GMP MNC-sec rad (the equivalent of 5×10^6 MNCs). Afterwards, six animals were anesthetized deeply with xylazine (10 mg/kg) i.p. and ketamine (100 mg/kg) i.p. after 2, 12 and 24 h (three animals for the MNC-sec rad group and three for Medium), and the inferior vena cava of each animal was punctured to draw blood. This draw was followed by a deep heart incision. The obtained blood samples were centrifuged at 3500 *g* for 15 min to obtain serum.

Statistical analysis

Statistical analysis was performed using GRAPHPAD PRISM4 software (GraphPad Software, La Jolla, CA, USA). Comparisons between groups at given time points were tested by Student's *t*-test. Data are represented as mean ± standard deviation (SD). Differences were also assessed graphically using bars and symbol connection lines. The calculations were performed separately for each experimental setting. A two-sided corrected P-value < 0·05 was considered significant.

Results

Antimicrobial activity of MNC-sec against Gram-negative and Gram-positive bacteria

To investigate whether irradiation of MNCs augments antimicrobial activity, we performed an antimicrobial microdilution assay with MNC-sec from irradiated and non-irradiated white blood cells. We observed increased antimicrobial activity of the secretomes derived from MNCs 24 h after irradiation (Fig. 1).

As shown in Fig. 1a, growth of the Gram-negative bacterium *P. aeruginosa* was significantly inhibited by both, MNC-sec rad (71 ± 21) and MNC-sec (14 ± 14; Medium as negative control, 0 ± 0% inhibition; all mean ± SD: Medium vs. MNC-sec rad, $P = 0·0001$; Medium vs. MNC-sec, $P = 0·03$). In contrast, the Gram-negative bacterium *E. coli* (Fig 1b) was also significantly inhibited by MNC-sec rad (66 ± 32) but not by MNC-sec (9 ± 16; Medium as negative control, 0 ± 0% inhibition; all mean ± SD: Medium vs. MNC-sec rad, $P = 0·0005$; Medium vs. MNC-sec, $P = 0·24$). In addition, we also found a

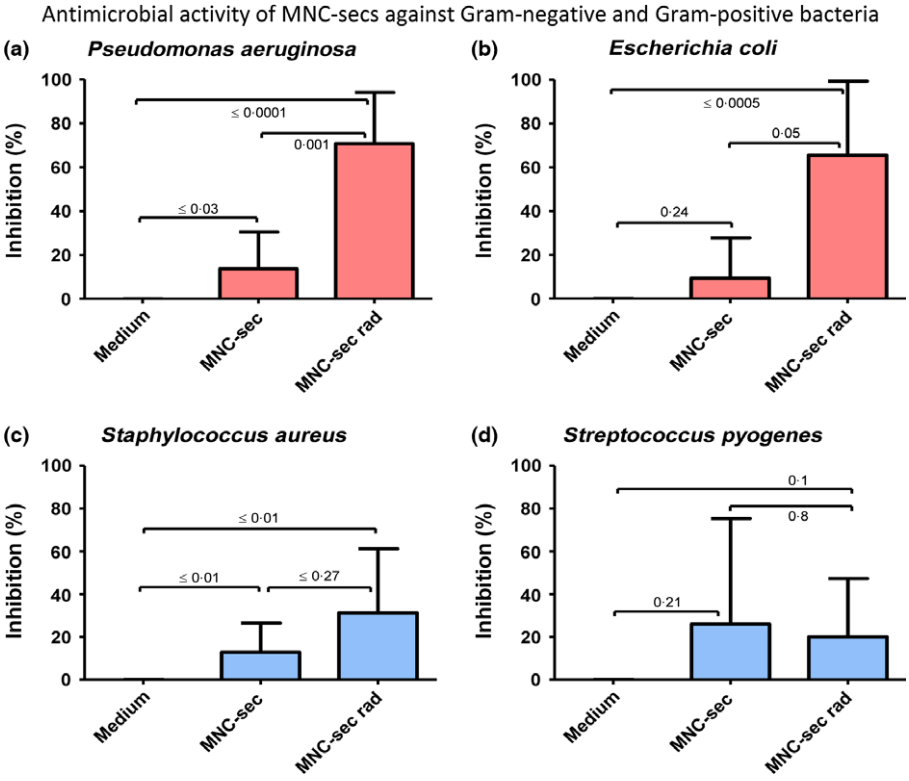

Figure 1 Antimicrobial activity of irradiated and nonirradiated MNC-sec against Gram-positive (blue bars) and Gram-negative (red bars) bacteria, presented data are mean ± SD of nine independent experiments shown as percentages of inhibition. Medium served as control. We show more than 70% inhibition of (a) *P. aeruginosa* growth and more than 60% significant inhibition of (b) *E. coli* growth compared to control (medium). Furthermore, we show up to 30% significant inhibition of (c) *S. aureus* growth and more than 20% insignificant inhibition of (d) *S. pyogenes* growth compared to medium. *P* values ≤ 0·05 were considered statistically significant. All MNC-sec are obtained 24 h after incubation of irradiated and nonirradiated MNCs.

significant growth inhibition of the Gram-positive bacterium *S. aureus* (Fig. 1c) treated with MNC-sec rad (31 ± 28) and MNC-sec (13 ± 12, mean ± SD; Medium as negative control, 0 ± 0% of inhibition, mean ± SD; Medium vs. MNC-sec, $P = 0{\cdot}01$, Medium vs. MNC-sec rad, $P = 0{\cdot}01$). Growth of *S. pyogenes* was only weakly inhibited by both secretomes (Fig. 1d) without reaching statistical significance (Medium vs. MNC-sec, $P = 0{\cdot}1$ and Medium vs. MNC-sec rad, $P = 0{\cdot}21$, respectively).

These results suggest that irradiation of MNC-sec significantly augments the antimicrobial activity against Gram-negative (*P. aeruginosa and E. coli)* and Gram-positive (*S. aureus)* bacteria, each of which important pathogens in DFU.

Gamma-irradiation of MNCs induces early apoptosis and necroptosis

To study how and to which extend MNCs are dying after exposure to γ-radiation, we next performed imaging flow cytometric analysis with ImageStream technology. In previous studies, we were able to show that 24 h after irradiation a huge substantial proportion of MNCs were Annexin V and PI double positive, leading to an increased secretory phenotype of the cells [22,26.] However, using conventional flow cytometry, we were not able to discriminate between late apoptosis and necroptosis. Using automated high-throughput morphological image analysis (ImageStream), we found that the dying cells displayed early apoptotic (26·1%) and necroptic (14·8%) phenotypes (Fig. 2). Early apoptotic cells expose phosphatidylserine on the cell surface, followed by membrane blebbing, nuclear fragmentation and decreased cell volume in late apoptotic cells [27]. In contrast, cells undergoing programmed necrosis show early plasma membrane rupture and fast cytoplasmic and nuclear swelling [28]. Compared to untreated cells (Fig. 2a), we found a strong increase in Annexin V and PI double-positive cells in γ-irradiated MNCs (Fig. 2b,c). Using the algorithm recently described by Pietkiewicz *et al* [23.], we could show that within the Annexin V and PI double-positive cell population 95% showed morphological features described for necroptotic cell death (Fig. 2d).

Irradiated and nonirradiated MNCs express and release antimicrobial peptides

To investigate whether MNCs express antimicrobial peptides, we performed RT-PCR at 0, 4 and 24 h after irradiation and cultivation. We showed a significant increase in angiogenin/RNase5 mRNA levels in irradiated MNCs compared to nonirradiated after 24 h (Fig. 3a; fold change, all mean ± SD, 15·7 ± 1 vs. 6·4 ± 2, $P = 0{\cdot}001$). Cathelicidin mRNA was also expressed in irradiated as well as nonirradiated MNCs and remained quite stable during the time course (Fig. 3b). Gene

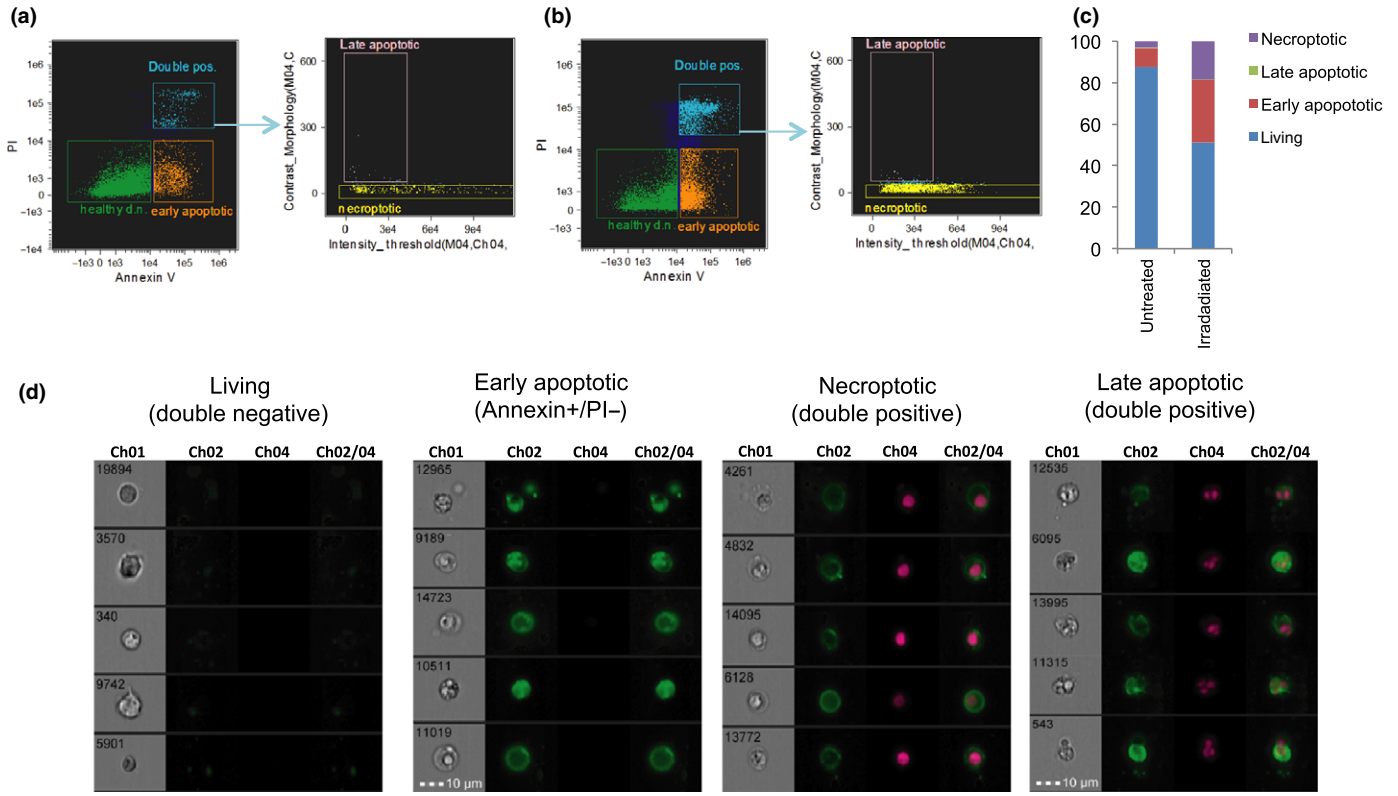

Figure 2 Analysis of the type of cell death. The type of cell death was investigated on MNCs 24 h after exposure to γ-radiation by ImageStream analysis. To detect the percentage of early and late stages of programmed cell death, the cells were stained with annexin V and propidium iodide. FACS analyses of nonirradiated (a) and irradiated (b) MNCs 24 h after γ-irradiation are shown. Viable cells are annexin V and propidium iodide-negative (lower left quadrant), whereas early apoptotic cells are annexin V-positive and propidium iodide-negative (lower right quadrant) and late apoptotic or necroptotic cells are double positive (upper right quadrant). (c) The percentages of the different cell states are show. (d) High-throughput morphological image analysis allows a clear discrimination between living, early apoptotic, late apoptotic and necroptotic cells. Channel 1 (Ch01) shows a light microscopical picture of the cells. Channel 2 (Ch02) shows the green fluorescence staining with Annexin V, channel 4 (Ch04) shows the red fluorescence staining with PI and channel 2/4 (Ch02/04) shows a merged picture of Ch2 and Ch3. One representative experiment of two is shown.

expression analysis of RNase7 decreased within the first 4 h and remained quite stable until 24 h (Fig. 3c). Interestingly, the mRNA expression level of S100A9 decreased in a time-dependent fashion (Fig. 3d). In addition, we analysed the gene expression of human β-defensins 1, 2, 3 and S100A7 and identified no expression in the irradiated or nonirradiated MNC gene pool (data not shown).

To further investigate AMP production on the protein level, we measured the concentration of released AMPs in the supernatant of both irradiated and nonirradiated MNCs after 4 and 24 h (Fig. 3e,f). Although S100A9 mRNA were decreases after 24 h, we found a significant released amount of calprotectin (a dimer of S100A8 and S100A9; Fig. 3e) and cathelicidin (Fig. 3f) after 24 h of culture. Furthermore, irradiation of MNCs further augmented calprotectin release (Fig. 3e; $P \leq 0{\cdot}0002$). Released Angiogenin/RNase 5 protein was not detected in either irradiated or nonirradiated MNC-sec. In addition, we detected high amounts of RNase3 and human beta-defensin 124 in irradiated MNC-sec, two proteins with putative, however so far unknown antimicrobial activity (Appendix 2). Blocking of the two major AMPs (calprotectin and Angiogenin/RNAse5) did not abrogate the antimicrobial activity (Appendix 3).

Presence of AMPs in irradiated MNC-sec produced according to the GMP protocol

The next aim was to investigate whether antimicrobial factors are present in our envisioned final drug product for the

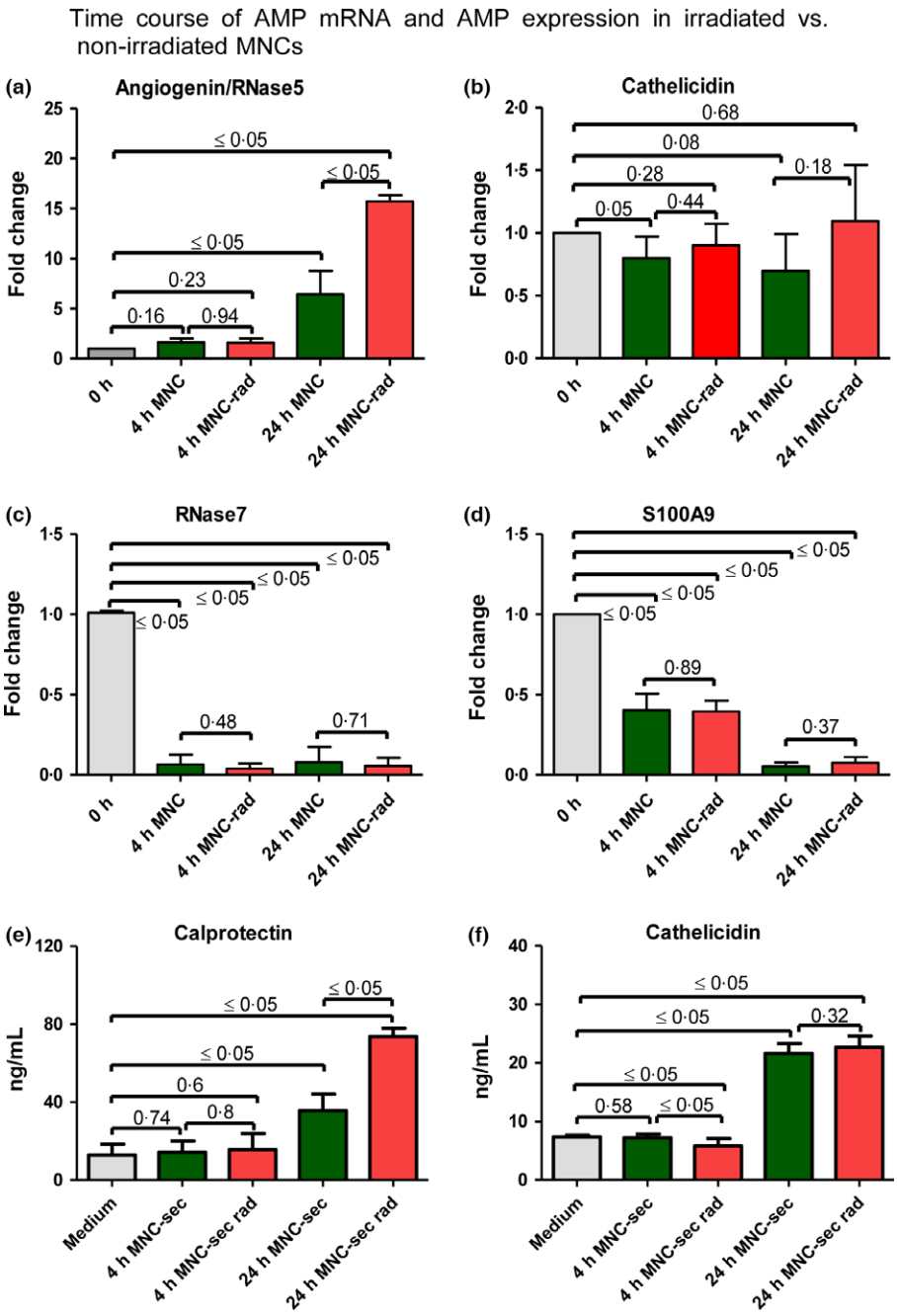

Figure 3 mRNA expression levels of selected AMPs and time course of AMP expression in MNC-sec. The AMPs were selected based on the coverage of different expression levels. The cohort for RT-PCR validation consisted of five patients. Cell culture supernatants derived from irradiated and nonirradiated MNCs ($n = 4$) were collected after 4 and 24 h. The levels of AMPs were evaluated by ELISA. Medium served as control. P values $< 0{\cdot}05$ were considered statistically significant. (a) Significantly higher angiogenin/RNase5 gene expression was detected in the supernatant of irradiated compared to nonirradiated MNCs after 4 h of increase in a time-dependent manner. (b) High levels of cathelicidin gene expression were detected in irradiated and nonirradiated MNCs with a tendency to an insignificant increase in irradiated MNCs. (c) Gene expression of RNase7 was highest at the beginning and decreased within the first 4 h and remained quite stable until 24 h. (d) Gene expression of S100A9 was highest at the beginning and decreased in a time-dependent manner within the first 4 h. (e) Irradiation of MNCs induced higher calprotectin release in the supernatant of irradiated MNCs after 24 h. (f) the concentration of cathelicidin increased significantly in the supernatant of both irradiated and nonirradiated MNCs in a time-dependent manner.

treatment of DFU. Cathelicidin, calprotectin, RNase3 and human beta-defensin 124 were determined to be present in concentrations similar to those of experimental non-GMP-manufactured MNC-sec. These data indicated that the twofold measure of viral clearance (methylene blue and high-dose gamma-irradiation at 25 000 Gy) did not alter AMP content in the final drug product (Table 1).

GMP MNC-sec stimulates endogenous AMP production in rats

To further explore whether GMP MNC-sec induces *de novo* AMPs *in vivo*, we injected human MNC-sec into rats and investigated plasma levels of rat calprotectin at 2, 12 and 24 h. These experiments were similar to those performed by Altmann *et al.* and

Table 1 Concentrations of AMPs in human experimental- and GMP-irradiated MNC-sec (pooled)

AMPs	GMP MNC-sec ng/ml	Experimental MNC-sec ng/ml
Cathelicidin	24·75 ± 5	22 ± 1
Calprotectin	82·25 ± 4	73 ± 4
RNase 3	19·75 ± 3	9 ± 5
DEFB 124	2·75 ± 1	6 ± 1

AMP levels were measured by ELISA. Data are mean ± SD of four independent experiments.

Haider *et al.* showing that human MNC-sec induced *de novo* rat brain-derived neurotrophic factor and CXCL1 chemokine [18,29]. Rat calprotectin concentration was measured by rat-specific ELISA, and we found a highly elevated level of rat calprotectin 24 h after i.p. administration of irradiated MNC-sec (1849 ± 495 compared to 0 h, 404 ± 32; $P = 0{\cdot}007$). This increase was highly significant compared to the Medium group after 24 h (362 ± 66; $P = 0{\cdot}007$), indicating that xenogeneic MNC-sec induces secretion of rat AMPs *in vivo* (Fig. 4).

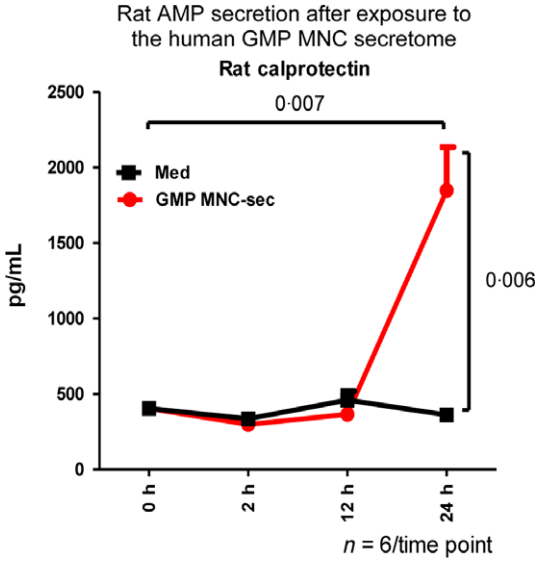

Figure 4 Time course of AMP expression in rat serum ($n = 6$/time point). Secretome MNCs derived from irradiated MNCs after 24 h were injected into healthy male rats. Rat serum samples were obtained at 2, 12 and 24 h after injection. AMP levels were measured by rat-specific ELISAs. A highly significant increase in rat calprotectin 24 h after injection of irradiated MNC-sec compared to medium was detected. All values are shown as mean ± SD. P values < 0·05 were considered statistically significant.

Discussion

DFU is a major complication of diabetes mellitus with a huge economic burden. Because wound healing is a dynamic and complex process with multifactorial aetiology, the management of DFU requires different actions, including debridement when necessary, optimal control of blood glucose, antibiotic therapy [30]. However, despite all of the efforts made, 14–20% of patients with DFU end up with amputation [31], and more than 50% of those amputees have less than 5-year survival rates [32].

Our group previously demonstrated the regenerative properties of MNC-sec rad. The therapeutic effects of MNC-sec rad include inhibition of microvascular obstruction, vasodilation [16], angiogenesis, enhanced migration of human primary keratinocytes and fibroblasts, reduction in scar formation after burn injury [21] and improvement of wound healing [19], all of which play major roles in wound-healing mechanisms. Here, we investigated whether antimicrobial activity is also a property of MNC-sec because it is well known that infection complicates treatment of DFU and is responsible for at least half of the cases of lower limb amputations [33]. Until recently, only scarce evidence had been published indicating that MNCs secrete AMPs and thus demonstrate antimicrobial activity in functional assays [20,30]. The special focus of our study was on the investigation of the antimicrobial properties of MNC-sec rad which is produced under GMP conditions including a twofold measure of viral clearance (methylene blue and high-dose gamma-irradiation at 25 000 Gy).

Our findings provide the first evidence that high-dose gamma-irradiation, inducing cell death, has a positive effect on AMP production and secretion of MNCs. Which pathway of cell death accounts for the observed effects of MNC-sec rad is an interesting but still open question. Approximately 50% of the irradiated cells enter a form of programmed cell death. Interestingly, this high dose of ionizing radiation induced early apoptosis, followed by necroptosis. This finding is of particular interest as we have shown previously that γ-irradiation indeed induces a secretory phenotype in MNCs [26] which might be due to the induction of necroptosis. Our data suggest that a very complex interplay between several different forms of cell death contributes to the observed positive activities of MNC-sec rad. The exact mechanisms, however, are still not known and our study builds a basis for future investigations.

In addition, we could demonstrate for the first time that MNC-sec rad displays a direct antimicrobial activity. In particular, the growth of Gram-negative *P. aeruginosa* and *E. coli.* and Gram-positive *S. aureus* was considerably reduced by incubation of these pathogens with the secretome of irradiated MNCs, and to a significantly lesser degree, with the secretome of nonirradiated MNCs. As for the source of this antimicrobial activity, a high abundance of different AMPs was found in the

conditioned medium. Interestingly, blocking two major AMPs present in our secretome did not abrogate its antimicrobial activity, suggesting multifactorial components accounting for the observed bactericidal action of the secretomes. This is in line with one of our previous studies, were we demonstrated that blocking the major survival factors (VEGF, IL-8, ENA-78) with blocking antibodies was not sufficient to abolish the cytoprotective activity of the secretome [34]. In our exploration, we showed a significant enhancement of antibacterial activity of irradiated MNC-sec. In respect to DFU and its potential favourable treatment with MNC-sec, *Pseudomonas* and *S. aureus* are most frequently found in this disease entity [35]. In addition, we also showed a significant increase in the antibacterial activity of irradiated MNC-sec against Gram-negative *E. coli* as compared to nonirradiated MNC-sec. The potential use of MNC-sec for systemic and topical treatment of *S. aureus* relates to the fact that a wide variety of human illnesses, ranging from relatively benign soft tissue infections to life-threatening toxic shock syndrome, necrotizing pneumonia and infective endocarditis, is still in need of alternative treatment options [36,37].

To further substantiate the presence of antimicrobial components in MNC-sec, we performed gene expression analyses that were validated by ELISA at the protein level. RT-PCR validation of angiogenin/RNase5 showed that irradiation led to a massive increase in mRNA production after 24 h ($P < 0{\cdot}0001$). These results supported our primary hypothesis that irradiation causes increased AMPs in MNC-sec. Despite high mRNA expression, we were not able to detect angiogenin/RNase5 at the protein level in our MNC-sec, suggesting that high amounts of the protein are stored intracellularly. For the release of the protein further triggers, such as pathogen recognition, might be necessary. However, to fully elucidate this mechanism, further experiments are needed.

Cathelicidin mRNA was also expressed in both irradiated and nonirradiated MNCs, findings that were corroborated using a commercially available ELISA system to verify protein release. This finding was of particular interest as cathelicidin has been previously identified as the responsible factor in the antimicrobial activity of MSC secretomes [9].

In addition, we found high levels of secreted calprotectin in irradiated MNC-sec. Interestingly, while secreted calprotectin protein was increasing, calprotectin mRNA decreased in a time-dependent manner. This might represent a mechanism by which rapid antimicrobial action is provided, but overproduction leading to strong inflammatory reactions is tempered by downregulation of mRNA production. A similar mechanism could also account for RNase7. However, due to technical limitations, we were only able to analyse RNase7 expression on the mRNA level. The exact underlying mechanisms remain to be elucidated.

It should be emphasized that the analysed substance contained the secretome of 25×10^6 MNCs. However, as previously described [20], we obtained the supernatant of 250×10^6 cells for the microdilution assay. Therefore, we argue that the effective concentration of soluble AMPs in MNC-sec is far beyond that measured.

In spite of the limited information about the role of AMPs in the pathogenesis of DFU, β-defensins are known to be overexpressed in DFUs, whereas the AMP cathelicidin shows low or no expression in comparison with healthy skin. These data suggest that possible MNC-sec treatment in DFU, containing cathelicidin and others (calprotectin, RNase3, DEFB124), would be an appropriate measure to promote wound healing by preventing secondary infections [5].

In the setting of topical and systemic infection, autochthonous production of AMPs would be a most desired effect in MNC-sec-treated patients because AMPs are well characterized and include recruitment of macrophages, granulocytes and lymphocytes like T cells by α-defensins [38–40] or chemotactic activity of cathelicidin with the highest affinity for CD4 T cells [20].

Our findings revealed that naive rats exposed to xenogeneic GMP MNC-sec showed a marked increase in rat calprotectin in a time-dependent fashion. Thus, we present here for the first time compelling evidence that MNC-sec rad can stimulate the secretion of endogenous AMPs *in vivo*. Whether or not irradiation of MNCs is indeed necessary to induce endogenous AMP expression remains to be elucidated.

Taken together, our results suggest that *in vitro* and *in vivo* effects on vascularization and wound healing can be associated with angiogenic and antimicrobial/chemotactic AMPs like cathelicidin [41]. Furthermore, we provide strong evidence that MNC-sec rad can have direct and indirect positive effects on the immune system, including exerting antibacterial properties.

Acknowledgements

The Christian Doppler Research Association provided funding for manuscript editing. We thank Ionela-Mariana Nagelreiter for technical help with the image stream analysis.

Disclosure

The Christian Doppler Research Association, APOSCIENCE AG and the Medical University of Vienna funded this study (Patent number: PCT/EP09/67534, filed 18 Dec 2008; Patent name: Pharmaceutical Preparation Comprising Supernatant of Blood Mononuclear Cell Culture). H.J. Ankersmit is a shareholder of APOSCIENCE AG, which owns the rights to commercialize MNC-sec for therapeutic use. All other authors declare that they have no competing financial interest.

Address
Christian Doppler Laboratory for Cardiac and Thoracic Diagnosis and Regeneration, Vienna, Austria (M. M. Kasiri, L. Beer, T. Haider, E. M. Simader, D. Traxler, S. Janik, H. J. Ankersmit); Department of Biomedical Imaging and Image-guided Therapy, Medical University of Vienna, Vienna, Austria (L. Beer); Division of Thoracic Surgery, Medical University of Vienna, Vienna, Austria (L. Nemec, T. Schweiger, S. Taghavi, H. J. Ankersmit); Department of Dermatology, Medical University of Vienna, Vienna, Austria (F. Gruber, M. Mildner); Christian Doppler Laboratory for Biotechnology of Skin Aging, Vienna, Austria (F. Gruber); Translational Inflammation Research, Otto von Guericke University, Magdeburg, Germany (S. Pietkiewicz); Red Cross Blood Transfusion Service of Upper Austria, Linz, Austria (C. Gabriel); Head FFG Project 852748 'APOSEC', Medical University of Vienna, Vienna, Austria (H. J. Ankersmit).

Correspondence to: Hendrik Jan Ankersmit, MD, Department of Thoracic Surgery, Medical University of Vienna, Christian Doppler Laboratory for Cardiac and Thoracic Diagnosis and Regeneration, Währinger Gürtel 18-20, 1090 Vienna, Austria.
Tel.: +43 1 40400 67770; fax: +43 1 40400 69770; e-mail: hendrik.ankersmit@meduniwien.ac.at
and
Michael Mildner, PhD, Division of Biology and Pathobiology of the Skin, Department of Dermatology, Medical University of Vienna, Research, Lazarettgasse 14, 1090 Vienna, Austria.
Tel.: +43 1 40400 73507; fax: +43 1 40400 73590; e-mail: michael.mildner@meduniwien.ac.at

Received 14 September 2015; accepted 9 August 2016

References

1 Gudmundsson GH, Agerberth B. Neutrophil antibacterial peptides, multifunctional effector molecules in the mammalian immune system. *J Immunol Methods* 1999;**232**:45–54.
2 Niyonsaba F, Iwabuchi K, Someya A, Hirata M, Matsuda H, Ogawa H *et al.* A cathelicidin family of human antibacterial peptide LL-37 induces mast cell chemotaxis. *Immunology* 2002;**106**:20–6.
3 da Costa JP, Cova M, Ferreira R, Vitorino R. Antimicrobial peptides: an alternative for innovative medicines? *Appl Microbiol Biotechnol* 2015;**99**:2023–40.
4 Reddy KV, Yedery RD, Aranha C. Antimicrobial peptides: premises and promises. *Int J Antimicrob Agents* 2004;**24**:536–47.
5 Rivas-Santiago B, Trujillo V, Montoya A, Gonzalez-Curiel I, Castañeda-Delgado J, Cardenas A *et al.* Expression of antimicrobial peptides in diabetic foot ulcer. *J Dermatol Sci* 2012;**65**:19–26.
6 Vu BG, Stach CS, Salgado-Pabón W, Diekema DJ, Gardner SE, Schlievert PM. Superantigens of *Staphylococcus aureus* from patients with diabetic foot ulcers. *J Infect Dis* 2014;**210**:1920–7.
7 Ho TK, Leigh RD, Tsui J. Diabetic foot disease and oedema. *Br J Diabetes Vasc Dis* 2012;**13**:45–50.
8 Waniczek D, Kozowicz A, Muc-Wierzgoń M, Kokot T, Świętochowska E, Nowakowska-Zajdel E. Adjunct methods of the standard diabetic foot ulceration therapy. *Evid Based Complement Alternat Med* 2013;**12**:243568.
9 Krasnodembskaya A, Song Y, Fang X, Gupta N, Serikov V, Lee JW *et al.* Antibacterial effect of human mesenchymal stem cells is mediated in part from secretion of the antimicrobial peptide LL-37. *Stem Cells* 2010;**28**:2229–38.
10 Wu Y, Chen L, Scott PG, Tredget EE. Mesenchymal stem cells enhance wound healing through differentiation and angiogenesis. *Stem Cells* 2007;**25**:2648–59.
11 Ren G, Chen X, Dong F, Li W, Ren X, Zhang Y *et al.* Concise review: mesenchymal stem cells and translational medicine: emerging issues. *Stem cells Transl Med* 2012;**1**:51–8.
12 Maharlooeia MK, Bagheri M, Solhjoua Z, Jahromia BM, Akramib M, Rohanic L *et al.* Adipose tissue derived mesenchymal stem cell (AD-MSC) promotes skin wound healing in diabetic rats. *Diabetes Res Clin Pract* 2011;**93**:228–34.
13 Gnecchi M, He H, Liang OD, Melo LG, Morello F, Mu H *et al.* Paracrine action accounts for marked protection of ischemic heart by Akt-modified mesenchymal stem cells. *Nat Med* 2005;**11**:367–8.
14 Korf-Klingebiel M, Kempf T, Sauer T, Brinkmann E, Fischer P, Meyer GP *et al.* Bone marrow cells are a rich source of growth factors and cytokines: implications for cell therapy trials after myocardial infarction. *Eur Heart J* 2008;**29**:2851–8.
15 Ankersmit HJ, Hoetzenecker K, Dietl W, Soleiman A, Horvat R, Wolfsberger M *et al.* Irradiated cultured apoptotic peripheral blood mononuclear cells regenerate infarcted myocardium. *Eur J Clin Invest* 2009;**39**:445–56.
16 Hoetzenecker K, Assinger A, Lichtenauer M, Mildner M, Schweiger T, Starlinger P *et al.* Secretome of apoptotic peripheral blood cells (APOSEC) attenuates microvascular obstruction in a porcine closed chest reperfused acute myocardial infarction model: role of platelet aggregation and vasodilation. *Basic Res Cardiol* 2012;**107**:292.
17 Hoetzenecker K, Zimmermann M, Hoetzenecker W, Schweiger T, Kollmann D, Mildner M *et al.* Mononuclear cell secretome protects from experimental autoimmune myocarditis. *Eur Heart J* 2013;**36**:676–85.
18 Altmann P, Mildner M, Haider T, Traxler D, Beer L, Ristl R *et al.* Secretomes of apoptotic mononuclear cells ameliorate neurological damage in rats with focal ischemia. *F1000Res* 2014;**3**:131.
19 Mildner M, Hacker S, Haider T, Gschwandtner M, Werba G, Barresi C *et al.* Secretome of peripheral blood mononuclear cells enhances wound healing. *PLoS One* 2013;**8**:e60103.
20 Agerberth B, Charo J, Werr J, Olsson B, Idali F, Lindbom L *et al.* The human antimicrobial and chemotactic peptides LL-37 and alpha-defensins are expressed by specific lymphocyte and monocyte populations. *Blood* 2000;**96**:3086–93.
21 Hacker S, Mittermayr R, Mildner M, Haider T, Nickl S, Zimmermann M *et al.* Paracrine factors from irradiated peripheral blood mononuclear cells improve skin regeneration and angiogenesis in a porcine burn model. *Sci Rep* 2016;**6**:25168.
22 Beer B, Seemann R, Ristl R, Ellinger A, Kasiri MM, Mitterbauer A *et al.* High dose ionizing radiation regulates micro RNA and gene expression changes in human peripheral blood mononuclear cells. *BMC Genom* 2014;**15**:814.
23 Sabine P, Schmidt JH, Lavrik IN. Quantification of apoptosis and necroptosis at the single cell level by a combination of imaging flow

cytometry with classical annexin V/propidium iodide staining. *J Immunol Methods* 2015;**423**:99–103.
24 Pfaffl MW. A new mathematical model for relative quantification in real-time RT-PCR. *Nucleic Acids Res* 2001;**29**:e45.
25 Mildner M, Stichenwirth M, Abtin A, Eckhart L, Sam C, Gläser R *et al*. Psoriasin (s100a7) is a major Escherichia coli-cidal factor of the female genital tract. *Mucosal Immunol* 2010;**3**:602–9.
26 Beer L, Zimmermann M, Mitterbauer A, Ellinger A, Gruber F, Narzt MS *et al*. Analysis of the secretome of apoptotic peripheral blood mononuclear cells: impact of released proteins and exosomes for tissue regeneration. *Sci Rep* 2015;**5**:16662.
27 Krammer PH, Arnold R, Lavrik IN. Life and death in peripheral T cells. *Nat Rev Immunol* 2007;**7**:532–42.
28 Vandenabeele P, Galluzzi L, Vanden Berghe T, Kroemer G. Molecular mechanisms of necroptosis: an ordered cellular explosion. *Nat Rev Mol Cell Biol* 2010;**11**:700–14.
29 Haider T, Höftberger R, Rüger B, Mildner M, Blumer R, Mitterbauer A *et al*. The secretome of apoptotic human peripheral blood mononuclear cells attenuates secondary damage following spinal cord injury in rats. *Exp Neurol* 2015;**S0014-4886**:00081–3.
30 Edmonds M, Foster A. The use of antibiotics in the diabetic foot. *Am J Surg* 2004;**187**:25–8.
31 Yang M, Sheng L, Zhang TR, Li Q. Stem cell therapy for lower extremity diabetic ulcers: where do we stand? *Biomed Res Int* 2013;**2013**:462179.
32 Wukich DK, Hobizal KB, Brooks MM. Severity of diabetic foot infection and rate of limb salvage. *Foot Ankle Int* 2013;**34**:351–8.
33 Jeffcoate WJ, Harding KG. Diabetic foot ulcers. *Lancet* 2003;**361**: 1545–51.
34 Lichtenauer M, Mildner M, Hoetzenecker K, Zimmermann M, Podesser BK, Sipos W *et al*. Secretome of apoptotic peripheral blood cells (APOSEC) confers cytoprotection to cardiomyocytes and inhibits tissue remodelling after acute myocardial infarction: a preclinical study. *Basic Res Cardiol* 2011;**106**:1283–97.
35 Urvish T, Parameswaran S, Armstrong A, Burgueno Vega D, Griswold J, Dissanaike S *et al*. Prevalence of multiple antibiotic resistant infections in diabetic versus nondiabetic wounds. *J Pathog* 2014;**2014**:173053.
36 Lowy F. Staphylococcus aureus infections. *N Engl J Med* 1998;**339**:520–32.
37 Spaulding AR, Salgado-Pabón W, Kohler PL, Horswill AR, Leung DY, Schlievert PM. Staphylococcal and streptococcal superantigen exotoxins. *Clin Microbiol Rev* 2013;**26**:422–47.
38 Chertov O, Michiel DF, Xu L *et al*. Identification of defensin-1, defensin-2, and CAP37/azurocidin as T-cell chemoattractant proteins released from interleukin-8-stimulated neutrophils. *J Biol Chem* 1996;**271**:2935–40.
39 Yang D, Chertov O, Bykovskaia SN, Chen Q, Buffo MJ, Shogan J *et al*. Beta-defensins: linking innate and adaptive immunity through dendritic and T cell CCR6. *Science* 1999;**286**:525–8.
40 Welling MM, Hiemstra PS, van den Barselaar MT, Paulusma-Annema A, Nibbering PH, Pauwels EK *et al*. Antibacterial activity of human neutrophil defensins in experimental infections in mice is accompanied by increased leukocyte accumulation. *J Clin Investig* 1998;**102**:1583–90.
41 Salvado MD, Di Gennaro A, Lindbom L, Agerberth B, Haeggström JZ. Cathelicidin LL-37 induces angiogenesis via PGE2-EP3 signaling in endothelial cells, in vivo inhibition by aspirin. *Arterioscler Thromb Vasc Biol* 2013;**33**:1965–72.

Appendix 1

Bacterial microdilution essay protocol

To store bacterial colonies over a period of years we use glycerol/broth slurries stored at −80 °C. So we transport bacterial colonies from a Plate or a stab by a sterile plastic or metal loop into glycerol/broth slurry. Glycerol is a cryoprotectant, which will help the culture to survive under frozen conditions. These frozen cultures are stored at −80 °C and are used for 'plating out' colonies.

Plating out bacterial colonies

1 Place plates on bench top to let them come to room temperature.
2 Fetch the frozen glycerol/bacteria solution from freezer (never allow it to thaw).
3 Lightly scratch the surface of the frozen slurry by an inoculating loop.
4 Streak the loop all over the plate surface.
5 Incubate plates inverted at 37 °C overnight.

We can store streaked plates in a refrigerator for less than a week but for a bacterial assay it's important always to use freshly streaked colonies.

Bacterial assay procedure

1 Gently scrape off 2–4 bacterial colonies from the overnight incubated plates by a cotton swab.
2 Put the cotton swab into a 10 mL tube, resuspend with 10 mL 1% Tryptic Soy Broth (TSB) and vortex for 5 s.
3 Mix 100 μL of bacterial solution with 100 μL medium, MNC-sec or MNC-sec rad, and incubate for 3 h at 37 °C with shaking.
4 Dilute bacteria mixture 1 : 10 000 with 1% TSB and plate 100 μL on a Columbia Agar palte.
5 Incubate the the agar plates for 24 h at 37 °C.
6 Count the colonies on the next day.

Appendix 2

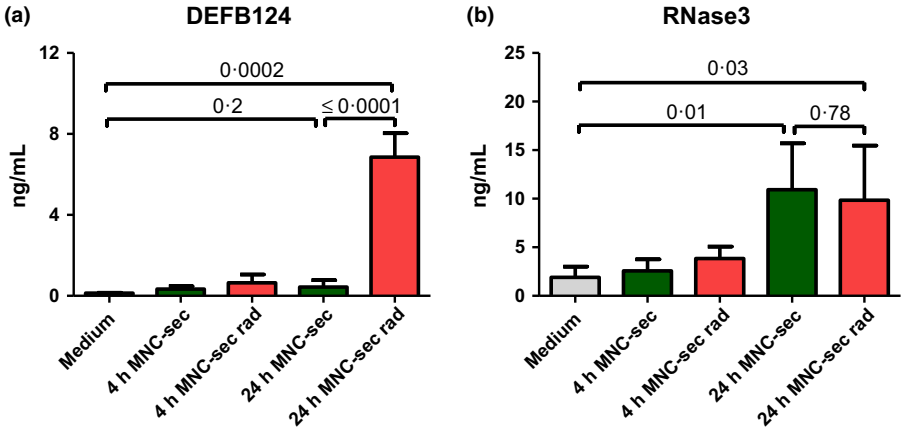

Time course of antimicrobial peptide expression in irradiated vs. non-irradiated MNC-sec. (n = 4), P values < 0·05 were considered statistically significant. Cell culture supernatants derived from irradiated and non-irradiated MNCs were collected after 4, and 24 h. The levels of AMPs were evaluated by ELISA. Medium served as control. (a) irradiation of MNCs induced higher DEFB124 release in the supernatant of irradiated MNCs after 24 h (P = 0·0002), significantly so compared to non-irradiated (P < 0·001); (b) the concentration of RNase3 increased significantly in the supernatant of both irradiated and non-irradiated MNCs in a time-dependent manner (P = 0·03, P = 0·01 respectively).

Appendix 3

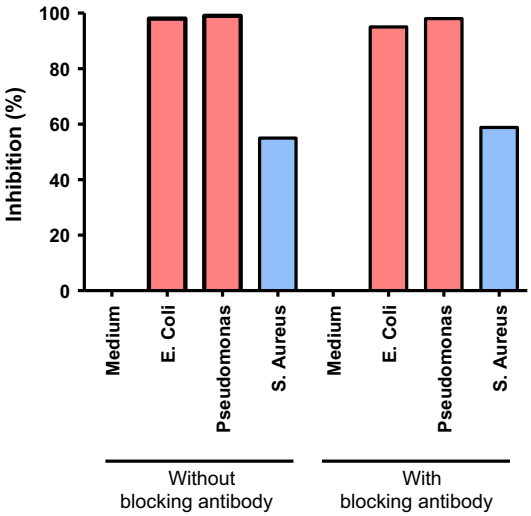

Blocking of antimicrobial peptides in irradiated MNC-sec. Antimicrobial activity of irradiated MNC-sec against Gram-negative and Gram-positive bacteria with and without blocking two of the major AMPs by neutralizing antibodies, presented data are one representative experiment of two (n = 1) shown as percentages of inhibition. Medium served as control. Blocking of the two major AMPs (Calprotectin and Angiogenin/RNAse5) did not abrogate the antimicrobial activity.